



Multiphase reactions of aromatic organosulfates with OH radicals: Kinetics, mechanisms, and environmental effects

Yu Yang¹, Caiqing Yan¹, Ruyu Yuang¹, Ping Liu¹, Hanyuan Zhang¹, Haibiao Chen¹, Yujiao Zhu¹, Hengqing Shen¹, Yan Wu², Likun Xue¹ and Liubin Huang^{1*}

¹Environment Research Institute, Shandong University, Qingdao, Shandong 266237, China ²School of Environmental Science and Engineering, Shandong University, Qingdao, Shandong 266237, China *Correspondence to*: Liubin Huang (hliubin@sdu.edu.cn)

Abstract. Aromatic organosulfates (aromatic OSs) are widely detected in the atmosphere and exhibit high abundance in urban areas. However, the atmospheric fate and environmental impacts of aromatic OSs remain poorly understood. In this study, we investigated the multiphase reaction of three aromatic OS (i.e., phenyl sulfate, p-tolyl sulfate, and 4-ethylphenyl sulfate) with OH radicals. The second-order reaction rate constant (k) of aromatic OSs with OH radicals were measured in the range of $4.29-6.38\times10^9$ M⁻¹ s⁻¹ at different pHs. It is found that k values are similar for the homologues of aromatic OSs, whereas are slightly affected by the solution pH values. The multiphase reactions of aromatic OSs and OH radicals mainly yield functionalized OSs, along with fragmented OSs and inorganic sulfate. The observation of inorganic sulfate formation, for the first time, indicates that aromatic OSs can also be converted into inorganic sulfate in analogues to aliphatic OSs. Furthermore, generated chromophores and fluorophores (constituents of brown carbon, BrC) products can significantly enhance the light absorption capacity, particularly under acidic conditions. These findings provide new insights into the understanding of the fate of aromatic OSs in the atmosphere that they can rapidly undergo atmospheric transformation, affecting the atmospheric sulfur cycle and altering aerosol optical properties.

20 1 Introduction

Secondary organic aerosols (SOA) play a significant role in regional air quality, climate change, and public health (Peng et al., 2023; Shrivastava et al., 2017; Liu et al., 2022). Organosulfates (OSs), organic compounds characterized by a sulfate ester functional group (R–O–SO₃⁻), have been widely detected in SOA in various environments (from remote to highly polluted) (Hansen et al., 2014; Kristensen et al., 2011; Zhang et al., 2012; Wang et al., 2018; Ma et al., 2025), accounting for ~30% of particulate organic mass (Surratt et al., 2008; Lukács et al., 2009; Tolocka and Turpin, 2012; Li et al., 2025). OSs can be produced from the reactions involving biogenic VOCs such as isoprene and monoterpenes, or anthropogenic VOCs such as diesel fuel vapor and aromatics (Wang et al., 2022; Thomas et al., 2025; Hettiyadura, et al., 2019; He et al., 2022). In the remote or clean areas, OSs were typically measured with the structure characterization of isoprene, monoterpenes, and their derivatives (Surratt et al., 2008; Zhang et al., 2012; Hettiyadura, et al., 2017). For example, Thomas et al. (2025) reported that IEPOX-OS (C₅H₁₂O₇S) is the dominant species of OSs in aerosols in Amazonian rainforest. In the urban areas, OSs containing



35

40



aromatic ring (e.g., phenyl sulfate, benzyl sulfate) were also ubiquitous in collected aerosols except for isoprene and monoterpenes derived OSs. Kundu et al. (2013) quantified the concentration of benzyl sulfate in the range of 0.05 to 0.5 ng m⁻³ in PM_{2.5} in Lahore, Pakistan, and also identified three additional methyl-substituted aromatic OSs (with $C_7H_7SO_4^-$ m/z 187, $C_8H_9SO_4^-$ m/z 201, and $C_9H_{11}SO_4^-$ m/z 215). Ma et al. (2014) reported that aromatic OSs accounted for up to 63.5% of the total identified OSs in Shanghai, China. These compounds seem to become more significant when anthropogenic VOCs appear to be the dominant source of SOA.

Extensive research has been conducted to elucidate the mechanisms of OSs in the atmosphere. The proposed formation mechanisms include: (a) the reactive uptake of epoxides on acidic sulfate aerosols. This pathway was established to be an important mechanism for the formation of isoprene-derived OSs (Surratt et al., 2010; Lin et al., 2013; Riva et al., 2019; Lei et al., 2022); (b) the multiphase reactions of either sulfate radicals or sulfur dioxide (SO₂) with unsaturated hydrocarbons (Nozière et al., 2010; Schindelka et al., 2013; Shang et al. 2016; Passananti et al. 2016). Previous studies revealed that the addition of sulfate radicals on the C=C bond can result in the formation of OSs in aqueous aerosols. Passananti et al. (2016) proposed that SO₂ can effectively react with unsaturated fatty acids to form OSs; (c) heterogeneous reaction of organic peroxides with SO₂. Recent laboratory studies have shown that SO₂ can also be oxidized by organic peroxides rapidly with the production of OS other than sulfate (Wang et al., 2019; Yao et al., 2019, 2023); (d) substitution reaction of organic nitrates (ONs) by sulfate (Darer et al., 2011; Hu et al., 2011). Darer et al. (2011) and Hu et al. (2011) observed the formation of OSs during the processes of ON hydrolysis in the presence of H₂SO₄; (e) acid-catalyzed esterification of alcohols. While laboratory studies reported OS formation from sulfate esterification (Iinuma et al., 2007), subsequent kinetic studies suggest this reaction is too slow under typical tropospheric conditions (Minerath et al., 2008).

Compared to the formation of OSs, understanding about the fate of OSs is still limited. Hydrolysis has been identified as a potential atmospheric removal process for certain OSs, with rates depending on the acidity of the aerosol and the molecular structure (Darer et al., 2011; Hu et al., 2011; Mael et al., 2015). Tertiary OSs were found to hydrolyze effectively under acidic conditions, while primary and secondary OSs were likely to be stable. Additionally, OSs can also further undergo the OH radical oxidation after they form. Lai et al. (2024) investigated the kinetics of OH radicals reacted with methyl sulfate and ethyl sulfate, finding that the reaction rate constant (k) may be significantly affected by the carbon chain length. k value of ethyl sulfate (3.8 \pm 0.1 \times 10⁸ L mol⁻¹ s⁻¹) was approximately five times higher than that of methyl sulfate (7.5 \pm 0.1 \times 10⁷ L mol⁻¹ s⁻¹). This observation was also verified in the border kind of aliphatic OSs (methyl sulfate, ethyl sulfate, and propyl sulfate) with the possible explanation of the inductive effects of the additional CH_x groups, which can enhance electron density at the H-abstraction site and stabilize the formed alkyl radical (Gweme and Styler, 2024). Chen et al. (2020a) detected the products of 2-methyltetrol sulfate diastereomers (IEPOX-OS) oxidized by OH radicals heterogeneously, observing varied fragmented and functionalized OSs after reactions, which their formation pathways were previously unknown in the atmosphere. Except for new OSs formed, previous study also pointed out that partial of OSs can return back to inorganic sulfate during the reaction of OH radicals with OSs (e.g., methyl sulfate, ethyl sulfate, and α -pinene derived OSs), indicating that it may potentially contribute to the atmospheric sulfur cycle (Kwong et al., 2018; Xu et al., 2020). It should be noted that

https://doi.org/10.5194/egusphere-2025-5606 Preprint. Discussion started: 25 November 2025





EGUsphere Preprint repository

the currently limited research about the fate of OSs focused on the biogenic OSs or small alkyl OSs, little is known about the kinetic and mechanism for the further conversion of aromatic OSs, which is another important kind of OSs, particularly in the urban aerosols. A very recent study investigated the aqueous phase OH radical oxidation of phenyl sulfate other than aliphatic OSs, they found that the rate of phenyl sulfate oxidized by OH radicals was much faster than that of aliphatic OS. After reactions, they observed the new OSs formed (hydroxyphenyl sulfate and dihydroxyphenyl sulfate), but without any evidence of inorganic sulfate production. However, whether aromatic OSs can be converted into inorganic sulfate or not remains unclear since they did not observe the presence of inorganic sulfate for aliphatic Oss as well. Therefore, to better characterize and understand the multiphase reaction of aromatic OS and OH radicals, further research is warranted.

In this study, we investigated the multiphase reaction of atmospherically relevant aromatic OSs (i.e., phenyl sulfate, p-tolyl sulfate, and 4-ethylphenyl sulfate) with OH radicals (He et al., 2022). Our study aims to explore the influence of substituent structure on reaction kinetics and elucidate the mechanism for the conversion pathways of aromatics in the atmosphere, and examine the change of optical properties.

2 Materials and methods

2.1 Batch reactor experiments

The aqueous oxidation of aromatic OSs was carried out in a 150 mL custom-built quartz reactor thermostated by a water jacket. The OH radical was generated through the aqueous photolysis of 10 mM H_2O_2 (30%, Hu Shi) under irradiation from a 300W Xenon arc lamp to simulate sunlight. Three commercial aromatic OSs, i.e., phenyl sulfate (\geq 98%, Macklin), p-tolyl sulfate (\geq 98%, Macklin), and 4-ethylphenyl sulfate (\geq 98%, Sigma-Aldrich), were used as representative aromatic OSs. Their structures were shown in Fig. S1. The reaction solution containing aromatic OS, H_2O_2 , and dissolved O_2 was introduced into the quartz reactor with a total volume of 100 mL, and was agitated by an electromagnetic stirrer. Subsequently, the reactor was sealed, and the xenon arc lamp was then ignited to start the reaction. Given that the pH of atmospheric water-containing particles typically ranges from 1 to 9 (Herrmann et al., 2015), the reaction solution was adjusted to pH 3 (using 36–38% HCl, Hu Shi) and pH 8 (using phosphate buffer (N_{12} 4 and N_{12} 4 PO₄)) to represent acidic and alkaline conditions, respectively. All experiments were performed at 298 K for $2\sim$ 12 h of reaction time. The initial concentration of OSs was 0.05 mM. Additional experiments with elevated concentrations of OSs (0.5 or 1 mM) were carried out in order to observe obvious product signals and optical change characteristics. Details about the information of the experiments carried out in this study are summarized in Table S1.

2.2 Kinetic measurements

The second-order rate constant of each aromatic OS with OH radical were measured by the competition kinetics methods that using sodium benzoate (BA, 98%, Macklin) as the reference (Smith et al., 2015). For the kinetic studies, 0.05 mM aromatic OS, BA, and 10 mM H₂O₂ were mixed in a quartz reactor, and the following reactions (R1 and R2) were conducted:



105

110



Aromatic OS +• OH
$$\rightarrow$$
 Products, k_{OS} (R1)

Reference
$$+ \bullet$$
 OH \rightarrow Products, k_{ref} (R2)

Assuming that aromatic OS and the reference compound are just consumed due to the OH radical oxidation in the aqueous phase, the second-order rate constant for aromatic OS (k_{OS}) can be calculated using the equation E1:

$$\ln\left(\frac{[OS]_0}{[OS]_t}\right) = \frac{k_{OS}}{k_{ref}}\ln\left(\frac{[ref]_0}{[ref]_t}\right) \tag{E1}$$

Where [OS] and [ref] are concentrations of aromatic OS and the reference compound (BA) during the experiment (time =0 and t). Time dependence of aromatic OS consumption was shown in Fig. S2. k_{ref} is the rate constant of BA with OH radicals, the values at pH 3 and 8 were reported as $4.3 \pm 0.8 \times 10^9 \,\mathrm{M}^{-1} \,\mathrm{s}^{-1}$ and $6.3 \pm 0.2 \times 10^9 \,\mathrm{M}^{-1} \,\mathrm{s}^{-1}$, respectively (Buxton et al., 1988). Figure 1 displays the relative kinetic plots for aromatic OSs oxidized by OH radicals under acidic (pH 3) and basic (pH 8) conditions. These plots exhibited strong linearity ($R^2 \ge 0.99$), with the slope of each linear fit corresponding to the k_{OS}/k_{ref} . According to the slopes and value of k_{ref} , the k_{OS} of the three aromatic OSs can be calculated. As the comparison, we also measured the rate of ethyl sulfate through this relative kinetic method. k_{OS} of ethyl sulfate was measured as $4.57 \pm 0.67 \times 10^8 \,\mathrm{M}^{-1} \,\mathrm{s}^{-1}$) that was measured at pH 9 (Gweme and Stylerl, 2024), further indicating the reliability of method employed in this study.

In order to eliminate the interference of other reactions to the kinetic process, two control experiments were also conducted: (1) a dark control under identical conditions except no illumination, and (2) a direct photolysis control under the same conditions but without the addition of H_2O_2 . As shown in Fig. S3 and S4, results of the dark reaction of H_2O_2 and the photolytic degradation experiments both exhibited a negligible influence on the concentrations of aromatic OSs.

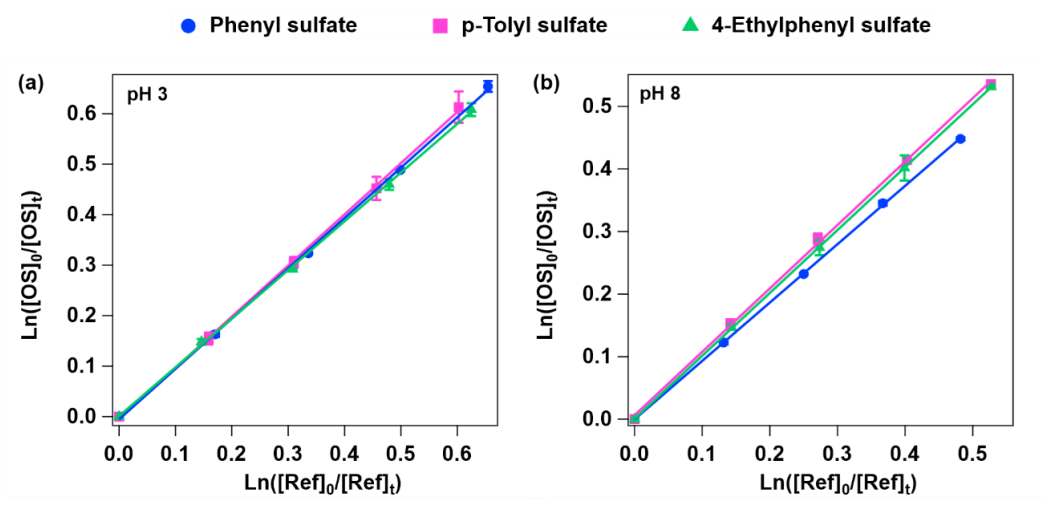


Figure 1. Loss of aromatic OSs and BA during the processes of the OH radical oxidation at (a) pH 3 and (b) pH 8.



115

120

125

130

135

140



2.3 Reactant and product analysis

The concentration of aromatic OSs and BA were detected using ultrahigh-performance liquid chromatography (UPLC, Agilent 1260) coupled with a UV detector operating at 254 nm. Separation was achieved on a ZORBAX Eclipse Plus C18 column (4.6 mm \times 250 mm, 5 μ m) maintained at 40 °C, with a mobile phase comprising acetonitrile and 0.1% formic acid (20:80, v/v) delivered at a flow rate of 0.8 mL min⁻¹. The injection volume was 10 μ L.

Ethyl sulfate and inorganic sulfate were analyzed by ion chromatography (Dionex ICS-600) with an analytical column (AS 11-HC, 4×250 mm; IonPac) and guard column (AG11-HC, $4 \text{ mm} \times 250$ mm, IonPac). The eluent was 20 mmol L⁻¹ potassium hydroxide at a flow rate of 1 mL min⁻¹.

The products were detected using an ultra-high performance liquid chromatography (UltiMate 3000) coupled to a Q Exactive ocus Hybrid Quadrupole-Orbitrap mass spectrometry (Thermo Scientific, USA). Separation was performed on a C18 column $(4.6 \text{ mm} \times 250 \text{ mm}, \text{ particle size} = 5 \mu\text{m}; \text{ZORBAX Eclipse Plus})$ at 40°C , with a binary mobile phase consisting of acetonitrile and 0.1% formic acid (20:80, v/v) delivered at a flow rate of 0.8 mL min⁻¹. Mass spectrometric detection was conducted in negative ionization mode over a mass range of 50-500 Da, with the spray voltage set at -3.0 kV, the capillary temperature at 320 °C, the S-lens RF level at -50V, the sheath gas (nitrogen) pressure at 2.76×10^5 Pa, and the auxiliary gas (nitrogen) flow rate of 3.33 L min⁻¹. Complementary analyses were carried out by a quadrupole time-of-flight mass spectrometry (O-TOF-MS, Bruker Impact HD, Germany) using the direct infusion mode under the negative ionization mode. The mobile phase consisted of pure water and acetonitrile (40/60 v/v) at a flow rate of 1 mL min⁻¹. The mass spectrometry was equipped with an electrospray ionization (ESI) source operated in the negative (-) ionization mode. The instrumental conditions for the (-) ESI-MS analysis were as follows: capillary voltage, 4000 V; gas temperature, 200 °C; dry gas flow rate, 5 L min⁻¹; and nebulizer pressure, 0.4 bar. Data were collected over the mass range of 50–500. Phenol generated in the experiment was verified by ultrahigh-performance liquid chromatography equipped with a fluorescence detector (UPLC-FLD). The fluorescence excitation and emission wavelengths were set at \(\lambda \text{ 220 nm and } \lambda \text{em 300 nm. A 10 } \mu L \text{ sample was injected into the instrument.} \) Separation was performed on a C18 column (4.6 mm × 100 mm, particle size = 2.7 μm; InfinityLab Poroshell) at 40 °C, eluting with a solution comprising pure water and acetonitrile (40/60 v/v) at a flow rate of 1 mL min⁻¹.

2.4 UV-vis absorption and fluorescent spectra

The light absorption spectra of samples during the processes of reactions were collected using a UV-vis spectrophotometer (DuettaTM, Horiba Scientific, Japan) with a scanning interval of 1 nm in the range of 250–700 nm. A reference absorption spectrum of hydrochloric acid solution (pH 3) or phosphate buffer solution (pH 8) was carried out in the same cuvette before sample analysis for baseline correction.

The excitation-emission matrix (EEM) fluorescence spectra were recorded by a fluorescence spectrometer (DuettaTM, Horiba Scientific, Japan). The excitation wavelength (Ex) and emission wavelength (Em) of EEM were both in the range of 250–600



155

160

165



nm. The scanning intervals were set to 5 nm and 2 nm. The solution with pH 3 or 8 was used as a blank to correct the data as well.

3 Results and discussion

3.1 Kinetics of multiphase reaction of aromatic OSs with OH radicals

Table 1 summarized the value of second-order rate constant (k_{OS}) for three aromatic OSs, i.e., phenyl sulfate, p-tolyl sulfate, and 4-ethylphenyl sulfate reacted with OH radicals. At pH 3, the k_{OS} value of phenyl sulfate was measured as $4.29 \pm 0.07 \times 10^9 \,\mathrm{M}^{-1} \,\mathrm{s}^{-1}$. This value is comparable to the literature result ($5.34 \pm 0.06 \times 109 \,\mathrm{M}^{-1} \,\mathrm{s}^{-1}$) reported by Gweme and Styler (2024), who investigated the k_{OS} of phenyl sulfate at pH 2 using pimelic acid as the reference. The slight difference may be attributed to the reference compound selection and the experimental conditions. Values of k_{OS} for other two OSs are similar to that of phenyl sulfate. The similar k_{OS} value among these three aromatic OSs suggests that the substituent carbon chain length on the aromatic ring has a negligible effect on the reaction kinetics. This is quite different from the alkyl OSs, which showed that k_{OS} is strongly dependent on the carbon number of OS contained (Lai et al., 2024; Gweme and Styler, 2024). Lai et al. (2024) reported that k_{OS} of ethyl sulfate was approximately five times higher than that of methyl sulfate. Gweme and Styler (2024) also found that k_{OS} value increased with increasing carbon chain length for methyl sulfate, ethyl sulfate, and propyl sulfate. This distinct behaviour may be ascribed to the different mechanism for aromatic OSs and alkyl OSs oxidized by OH radicals. For aromatic OSs, the OH radical predominantly attacks the aromatic ring with multiple addition sites and has high reactivity (Bloss et al., 2005; Garmash et al. 2020). While alkyl OSs react primarily through hydrogen abstraction, the increasing carbon chain length can enhance reactivity through the inductive effect of $-CH_x$ groups, the increasing electron density at the hydrogen abstraction site, and the stabilization of resulting alkyl radicals (Monod and Doussin, 2008;

Dorfman and Adams, 1973). As such, aromatic OS has high reactivity compared to alkyl OSs. The negligible effect of carbon number on the reactivity of aromatic compounds was also observed in other structure of homologue of aromatics. For example, previous studies reported similar rate constant for toluene $(8.1 \times 10^9 \text{ M}^{-1} \text{ s}^{-1})$ and benzene $(7.8 \times 10^9 \text{ M}^{-1} \text{ s}^{-1})$ with OH radicals (Schuler and Albarran, 2002). Notably, the k_{OS} value of aromatic OSs with the OH radical is lower than that of their parent aromatic hydrocarbons. This reduction in reactivity can be attributed to the electron-withdrawing effect of the $-\text{OSO}_3^-$ groups, which reduces the reactivity of the aromatic ring and the OH radical (Lai et al., 2024).

Table 1. The second-order rate constant (k) of aromatic OSs reacting with OH radicals in the aqueous phase at different pHs.

Species	k (10 ⁹ M ⁻¹ s ⁻¹)	
	pH = 3	pH = 8
Phenyl sulfate	4.29 ± 0.07	5.88 ± 0.01
p-Tolyl sulfate	4.36 ± 0.08	6.38 ± 0.16
4-Ethylphenyl sulfate	4.46 ± 0.04	6.33 ± 0.05
Benzoic acid ^a	4.3 ± 0.8	6.3 ± 0.2

^aRate constants for benzoic acid were obtained from Buxton et al. (1988)



175

180

185

190

195

200



Table 1 shows that the carbon chain length has an insignificant effect on the k_{OS} of aromatic OSs at pH 8 as well. k_{OS} values of phenyl sulfate, p-tolyl sulfate, and 4-ethylphenyl sulfate were calculated as $5.88 \pm 0.01 \times 10^9$, $6.38 \pm 0.16 \times 10^9$, and $6.33 \pm 0.05 \times 10^9$ M⁻¹ s⁻¹. It is noted that these values are higher than that of measured at pH 3. Gweme and Styler (2024) measured the k_{OS} of phenyl sulfate at pH 2 and pH 9, observing that it was the pH independence. They attributed this pH independence to phenyl sulfate remaining fully deprotonated (pKa = -2.2) across the entire experimental pH range. However, previous studies demonstrated that even though methoxyphenol, phenylglycol, and highly substituted phenol mainly exist in the form of protonation within the pH range of 2 to 6, their second-order reaction rate constants with OH radicals at pH 2 were generally lower than those at pH 5 or 6 (Arciva et al., 2022). This phenomenon may arise from several factors: (1) the acidic condition or high ionic strength could hinder OH radical attack on aromatic systems or reduce the lifetime of hydroxyl-cyclohexadienyl radical intermediates, slowing irreversible diol formation (Smith et al., 2015). (2) The uncertainty of the second-order rate constant of the reaction of reference with the OH radical (Arciva et al., 2022). Therefore, the difference and uncertainty of the rate constant of the reference may also be the reason for the discrepancy between Gweme and Styler (2024)'s and our study. Moreover, pronounced variations in product distributions under differing pH conditions imply the involvement of distinct reaction pathways. The mechanistic divergence likely serves as a key factor for the observed pH dependence of k_{OS} values.

3.2 Product measurements and reaction mechanism

Products of aromatic OSs after reaction were also detected by the mass spectrometer. Table S2 lists the products of the multiphase reaction of phenyl sulfate with OH at pH 3. The main signals were identified as hydroxyphenyl sulfate (C₆H₅O₅S⁻, m/z 189) and dihydroxyphenyl sulfate ($C_6H_5O_6S^-$, m/z 205), aligning with the literature result (Gweme and Styler, 2024). Additionally, the multiple OH radical addition products were also detected, including m/z 221 ($C_6H_5O_7S^-$) and m/z 237 (C₆H₅O₈S⁻). As illustrated in Fig. 2, the OH-initiated oxidation of phenyl sulfate follows a mechanism analogous to conventional aromatic compounds (e.g., benzene). The reaction initiates via the addition of an OH radical to the aromatic ring, generating hydroxycyclohexadienyl radicals (OH-PS radicals) (Lay et al., 1966; Minakata et al., 2015). OH-PS radicals rapidly react with O₂ to yield phenolic compounds that can undergo further multi-step OH radical additions to form these polyhydroxy products ($C_6H_5O_nS^-$, n=5-8). Alternatively, OH-PS radicals can also react with O_2 to form peroxyl radicals (RO₂ radical). The reversible cyclization of RO₂ radicals and the subsequent O₂ addition generate bicyclic peroxyl radicals. Bicyclic peroxyl radicals react with RO₂ radicald to produce ring-opening products as shown in Table S2 (Wang et al. 2013; Dong et al. 2021). Fragmented OS formation resulting from ring-opening pathway during OH oxidation of aromatic OSs has not reported previously, and partial of them (e.g., $C_2H_3O_5S^-$; $C_3H_5O_4S^-$, $C_3H_7O_5S^-$, $C_5H_5O_6S^-$) have the same formula of Oss detected in the atmosphere, which their precursors are still remain unidentified (Kuang et al., 2016; Cai et al., 2020; Huang et al., 2023) or are regarded as biogenic VOCs (Cai et al., 2020; Kuang et al., 2016; Wang et al., 2022). For example, m/z 139 (C₂H₃O₅S⁻) observed in this study was heretofore considered to be produced from isoprene and its derivates related reactions in the atmosphere (Cai et al., 2020; Wang et al., 2022). These findings suggest that aromatic OSs may serve as a potential source for aliphatic OSs.



215

220

225



$$\begin{array}{c} OH \\ + HSO_4 \\ + OH \\ \\ OSO_3 \\ + OH \\ \\ OH \\ OH \\ \\ OH \\$$

205 Figure 2. Scheme for the mechanism of phenyl sulfate reacting with OH radicals.

Intriguingly, in addition to the new OSs observed, the formation of inorganic sulfate (HSO₄-, m/z 97) was also detected. Previous studies revealed that partial of aliphatic OSs (e.g., methyl sulfate, ethyl sulfate, α -pinene-derived OS) can be converted into inorganic sulfate during OH oxidation. The molar yield of inorganic sulfate was estimated from 46±2% to 62±18% for the studied OSs (Lai et al., 2025; Xu et al., 2020). The oxidation mechanism of methyl sulfate is initiated through hydrogen abstraction from the alkyl group by OH radicals, forming an alkyl radical. The alkyl radical reacts rapidly with O2 to form the RO₂ radical. RO radicals, generating from the further reaction of RO₂ radical, can undergo β-scission to generate formaldehyde and sulfate anions (•SO₄⁻), thereby producing HSO₄⁻. In this study, the observation of a pronounced signal of at m/z 97 suggests that aromatic OSs can also return to inorganic sulfate, similar to aliphatic OSs. The result of the control experiment verifies that the pathway of phenyl sulfate hydrolysis can be excluded since the concentration of phenyl sulfate did not change within 2 h of reaction under the same conditions without UV (Fig. S3). It is noted that we also observed the formation of phenol in addition to inorganic sulfate (Fig. S5). Thus, the formation of inorganic sulfate is inferred to be produced from the elimination of the sulfate group from phenyl sulfate, as well as the ipso-addition followed by disproportionation reaction as shown in Fig. 2. Phenyl sulfate can also undergo ipso-addition to form OH-PS radical, the ipso-OH-adduct should either rapidly eliminate HSO₄⁻ accompanying with the formation of phenoxyl radical (precursor of phenol), or undergo bimolecular reactions with other isomer of the OH-PS radical to yield phenol upon elimination of HSO₄⁻ as well. However, compared to other OH addition pathways (o-add, m-add, and p-add), there is only very little room for the ipso-addition. It is noted that previous studies have shown that benzoic acid can undergo decarboxylation reactions. Another possible pathway for HSO₄ production is elucidated to be via the elimination of the sulfate group from phenyl sulfate as similar to the decarboxylation mechanism of benzoic acid. Unexpectedly, the yield of inorganic sulfate was measured as >80% using IC (Fig. S6). Although the peak of inorganic sulfate in IC was negligible at the beginning of reactions, we still cannot establish





that the peak of OS products in IC is not overlapped with the peak of inorganic sulfate. Thus, in this study, the yield of inorganic sulfate obtained from IC measurement is controversial, further investigation should be warranted. Nevertheless, the observation of inorganic sulfate in mass spectra for the first time implies that aromatic OSs can also be converted into inorganic sulfate in analogues to aliphatic Oss.

We also examined the effects of pH value on the mechanism of reactions. Figure S7 reveals that C₆H₅O₅S⁻ exists as three isomeric forms: ortho, meta, and para hydroxyphenyl sulfate, exhibiting distinct distribution patterns at different pH values. Additionally, the total abundance of C₆H₅O₅S⁻ was significantly higher at pH 8 compared to pH 3. This finding aligns with previous work by Pan et al. (1993), which uncovered that the primary product of phenol from the reaction of benzene and the OH radical shows dramatically increased yields (up to 93%) under alkaline conditions (pH 12.3). The pH-dependent product distribution observed in our study also evidences that the reaction mechanism of phenyl sulfate with OH radicals is significantly influenced by solution pH.

Similar to phenyl sulfate, the oxidation of p-tolyl sulfate and 4-ethylphenyl sulfate by OH radicals primarily yield phenolic compounds through OH-addition pathways, along with the fragmented products and inorganic sulfate. However, the presence of additional alkyl substituents in p-tolyl sulfate and 4-ethylphenyl sulfate enables alternative reaction pathways, in which OH radicals can abstract hydrogen atoms, leading to the formation of aromatic alcohols and aldehydes. (Baltaretu et al., 2009; Liu et al., 2017; Forstner et al., 1997).

3.3 Optical property changes

240

245

250

255

Kinetic and mechanism results show that aromatic OSs can proceed rapidly in OH oxidation to form a series of functionalized and fragmented compounds. Previous studies reported that multiphase oxidation of aromatic organic compounds often induces significant alterations in the optical properties of the reaction system (Li et al., 2021; Arciva et al., 2024). Thus, the change of optical properties during the process of aromatic OSs reacting with OH radicals was also monitored. Figure 3 shows the timedependent absorption spectra of aromatic OSs during OH radical oxidation at pH 3. As the reaction progressed, the depletion of precursor compounds correlated with a systematic increase in absorbance across 250-400 nm. The enhanced absorption at 250–300 nm corresponds to $\pi \to \pi^*$ transitions, likely indicative of newly formed aromatic C=C and carbonyl (C=O) functional groups (Li et al., 2022; Tang et al., 2020). Meanwhile, the observation of remarkable absorption at 300-400 nm, absent in the reactants, suggests the formation of light-absorbing brown carbon (BrC) species (Harrison et al., 2020; Laskin and Nizkorodov, 2015). The multiphase reaction of aromatic OS with OH radical generates polyhydroxyl substitution products. The electrondonating effect of hydroxyl groups elevates the electron density of the aromatic ring, inducing a redshift in the parent compound's absorption (Hems and Abbatt et al., 2018). Additionally, the generated BrC may originate from oligomers with large conjugated structures (Yu et al., 2014; Li et al., 2022). Although the three aromatic OSs exhibited similar trends in UV-Vis spectral evolution, there are still differences. For instance, the p-tolyl sulfate showed the most pronounced absorption enhancement at 260 nm, while the absorption peak of 4-ethylphenyl sulfate at 260 nm undergoes a blue shift, which is related to the different substituents of the reaction products.



270

275



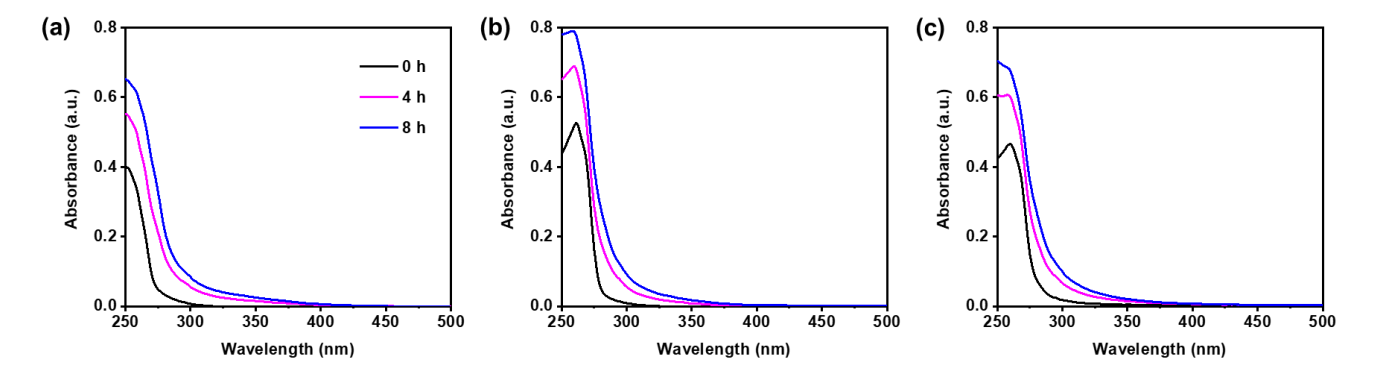


Figure 3. Time profile of UV-vis light absorption spectra during the processes of (a) phenyl sulfate, (b) p-tolyl sulfate and (c) 4-ethylphenyl sulfate reacting with OH radicals at pH 3.

Furthermore, the fluorescence characteristics of aromatic OSs during the multiphase oxidation were investigated using EEM fluorescence spectra. As shown in Fig. 4, the initial maximum excitation/emission (Ex/Em) wavelengths of phenyl sulfate, p-tolyl sulfate, and 4-ethylphenyl sulfate at pH 3 occurred at Ex/Em = 255/275 nm, 260/284 nm, and 260/284 nm, respectively. The different initial fluorescence intensity among these three aromatic OSs may be attributed to the substituent effect of the compound. Compared to phenyl sulfate, p-tolyl sulfate and 4-ethylphenyl sulfate contain additional methyl and ethyl groups, respectively. These electron-donating substituents extend the conjugation system, lowering the $\pi \rightarrow \pi^*$ transition energy and resulting in both emission redshift and fluorescence enhancement (Cao et al., 2023). During reactions, the fluorescence intensity initially decreased due to phenyl sulfate consumption, followed by a subsequent increase from fluorescent product formation. After 8 h of irradiation, a redshifted fluorescence peak emerged at Ex/Em = 260/283 nm, suggesting the formation of products with expanded conjugated systems (Tang et al. 2020). The fluorescence intensity of p-tolyl sulfate and 4-ethylphenyl sulfate monotonically decreases with the reaction time and shows a redshift in the fluorescence band at Ex/Em = (250-300)/(400-500). Previous studies suggest that the emission wavelengths of 400–500 nm are indicative of Humic-like substances (HULIS), which contribute to the light-absorbing properties of organic aerosols (Bianco et al., 2014). In addition, when non-photolyzable phenolic compounds are oxidized by OH radicals, yielding fluorescent products with spectral features resembling those of aerosol HULIS (Tang, et al., 2020; Chang et al., 2010).



285

290



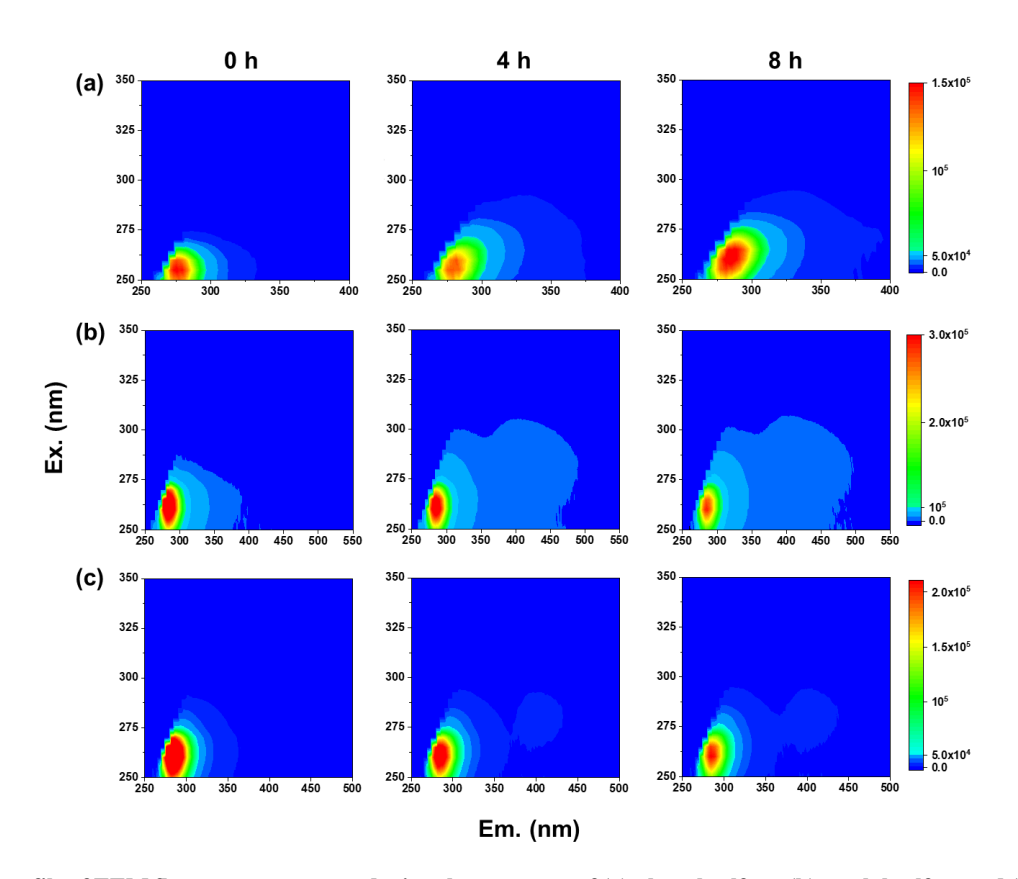


Figure 4. Time profile of EEM fluorescence spectra during the processes of (a) phenyl sulfate, (b) p-tolyl sulfate and (c) 4-ethylphenyl sulfate reacting with OH radicals at pH 3.

Employing phenyl sulfate as the representative, how the absorption spectra and EEM fluorescence spectra changed at pH 8 was also studied (Fig. S8 and S9). Previous studies have demonstrated that the light absorption properties of carbonyl compounds (e.g., aldehydes) and nitrophenols exhibit pronounced pH-dependence owing to protonation-deprotonation equilibria (Calvert and Schnitzler, 2023; Chen et al., 2020b). In this study, the phenyl sulfate remains deprotonated across the pH range of 3–8, resulting in negligible spectral variations in the initial solutions (Fig. 3 and S8). However, the temporal evolution of the reaction revealed substantially enhanced absorbance at pH 3 compared to pH 8, particularly within the 300–400 nm range. This pronounced difference suggests that low pH preferentially facilitates the formation of light-absorbing BrC species, likely through acid-catalyzed oligomerization (Heath and Valsaraj, 2013). Figure S9 reveals that phenyl sulfate exhibits an initial maximum fluorescence peak at Ex/Em = 255/279 nm at pH 8, showing minimal variation from the pH 3 condition. However, the temporal evolution of its fluorescence spectrum differs obviously between pH conditions. Under basic conditions (pH 8), we observed a monotonic decrease in fluorescence intensity without subsequent recovery, and no fluorescence peak redshift occurred even after 8 hours of reaction. This pH-dependent fluorescence behavior suggests distinct oxidation pathways under acidic versus basic conditions. The pronounced fluorescence redshift observed exclusively under acidic conditions further implies that larger, more conjugated photoproducts form preferentially under acidic conditions.



320



4 Atmospheric implications and conclusions

295 The current study investigates the multiphase reactions of aromatic OSs and OH radicals. The results of kinetic measurements indicate that aromatic OSs can undergo multiple reactions with OH radicals rapidly. As shown in Table S3, using the k value measured at pH 3 coupled with modeled OH radical concentrations (Herrmann et al., 2005, 2010), the corresponding lifetime $(\tau=1/k_{OS}\times[\bullet OH])$ of aromatic OS in urban aerosol and cloud was calculated to be 7 minutes and 16 h, respectively. The lifetime of aromatic OSs is significantly shorter than those of aliphatic OSs (Gweme and Styler, 2024; Lai et al., 2025). The formed 300 aromatics OSs can be transformed into functionalized and fragmented OSs as well as inorganic sulfate. Notably, the detection of alkyl OSs in the oxidation products challenges the conventional attribution of these compounds solely to biological sources, revealing aromatic OSs as an additional precursor in the atmosphere. Furthermore, the multiphase reaction of aromatic OSs with OH radicals generates functionalized OSs, which act as a BrC component to enhance light absorption, thereby influencing aerosol optical properties and perturbing radiative forcing. The high abundance and short atmospheric lifetime of aromatic OS 305 in urban environments further underscores their potentially significant role in both the atmospheric sulfur cycle and environmental effects. These findings establish that the multiphase reaction of aromatic OS with OH radical is a key transformation pathway and emphasize the significant impact of this pathway on urban aerosol chemistry and related climate effects.

310 Data availability. Data are available upon request from the corresponding author.

Author contributions. LH designed research. YY, CY RY, PL, HZ, and HC, performed research. YY and LH analyzed data. YY and LH wrote the paper. LX, CY, YW, YZ, and HS provided valuable comments and suggestions for the manuscript.

315 Competing interests. The contact author has declared that none of the authors has any competing interests.

Acknowledgements. This study was financially supported by the National Key Research and Development Program of China (2022YFC3701102), the National Natural Science Foundation of China (42207121), the Outstanding Young Scholar of the Natural Science Foundation of Shandong Province, China (Overseas) (2022HWYQ-010), the Natural Science Foundation of Shandong Province (ZR2024YQ046). Liubin Huang gratefully acknowledges the support of the Program for Taishan Young Scholar (tsqnz20221107).





References

340

- Arciva, S., Niedek, C., Mavis, C., Yoon, M., Sanchez, M. E., Zhang, Q., and Anastasio, C.: Aqueous ·OH oxidation of highly substituted phenols as a source of secondary organic aerosol, Environ. Sci. Technol., 56, 9959–9967, https://doi.org/10.1021/acs.est.2c02225, 2022.
 - Arciva, S., Ma, L., Mavis, C., Guzman, C., and Anastasio, C.: Formation and loss of light absorbance by phenolic aqueous SOA by •OH and an organic triplet excited state, Atmos. Chem. Phys., 24, 4473–4485, https://doi.org/10.5194/acp-24-4473-2024, 2024.
- Baltaretu, C. O., Lichtman, E. I., Hadler, A. B., and Elrod, M. J.: Primary atmospheric oxidation mechanism for toluene, J. Phys. Chem. A, 113, 221–230, https://doi.org/10.1021/jp806841t, 2009.
 - Bianco, A., Minella, M., Laurentiis, E. D., Maurino, V., Minero, C., and Vione, D.: Photochemical generation of photoactive compounds with fulvic-like and humic-like fluorescence in aqueous solution, Chemosphere, 111, 529–536, https://doi.org/10.1016/j.chemosphere.2014.04.035, 2014.
- Bloss, C., Wagner, V., Jenkin, M. E., Volkamer, R., Bloss, W. J., Lee, J. D., Heard, D. E., Wirtz, K., Martin-Reviejo, M., Rea, G., Wenger, J. C., and Pilling, M. J.: Development of a detailed chemical mechanism (MCMv3.1) for the atmospheric oxidation of aromatic hydrocarbons, Atmos. Chem. Phys., 5, 641–664, https://doi.org/10.5194/acp-5-641-2005, 2005.
 - Buxton, G. V., Greenstock, C. L., Helman, W. P., and Ross, A. B.: Critical review of rate constants for reactions of hydrated electrons, hydrogen atoms and hydroxyl radicals (•OH/•O- in aqueous solution, J. Phys. Chem. Ref. Data, 17, 513–886, https://doi.org/10.1063/1.555805, 1988.
 - Cai, D., Wang, X., Chen, J., and Li, X.: Molecular characterization of organosulfates in highly polluted atmosphere using ultra-high-resolution mass spectrometry, J GEOPHYS RES-ATMOS, 125, e2019JD032253, https://doi.org/10.1029/2019JD032253, 2020.
- Calvert, C. T., and Schnitzler, E. G.: Light absorption by cinnamaldehyde constituents of biomass burning organic aerosol modeled using time-dependent density functional theory, ACS Earth Space Chem, 7, 490–500, https://doi.org/10.1021/acsearthspacechem.2c00344, 2023.
 - Cao, T., Li, M., Xu, C., Song, J., Fan, X., Li, J., Jia, W., and Peng, P.: Technical note: Chemical composition and source identification of fluorescent components in atmospheric water-soluble brown carbon by excitation–emission matrix spectroscopy with parallel factor analysis potential limitations and applications, Atmos. Chem. Phys., 23, 2613–2625, https://doi.org/10.5194/acp-23-2613-2023, 2023.
 - Chang, J. L., and Thompson, J. E.: Characterization of colored products formed during irradiation of aqueous solutions containing H₂O₂ and phenolic compounds, Atmos. Environ., 44, 541–551, https://doi.org/10.1016/j.atmosenv.2009.10.042, 2010.
- Chen, Y., Zhang, Y., Lambe, A. L., Xu, R., Lei, Z., Olson, N. E., Zhang, Z., Szalkowski, T., Cui, T., Vizuete, W., Gold, A.,

 Turpin, B. J., Ault, A. P., Chan, M. N., Surratt, J. D.: Heterogeneous hydroxyl radical oxidation of isoprene-epoxydiol-



360

365



- derived methyltetrol sulfates: Plausible formation mechanisms of previously unexplained organosulfates in ambient fine aerosols, Environ. Sci. Technol. Lett., 7, 460–468, https://doi.org/10.1021/acs.estlett.0c00276, 2020a.
- Chen, J. Y., Rodriguez, E., Jiang, H., Chen, K., Frie, A., Zhang, H., Bahreini, R., and Lin, Y-H.: Time-dependent density functional theory investigation of the UV–Vis spectra of organonitrogen chromophores in brown carbon, ACS Earth Space Chem., 4, 311–320, https://doi.org/10.1021/acsearthspacechem.9b00328, 2020b.
- Darer, A. I., Cole-Filipiak, N. C., O'Connor, A. E., and Elrod, M. J.: Formation and stability of atmospherically relevant isoprene-derived organosulfates and organonitrates, Environ. Sci. Technol., 45, 1895–1902, https://doi.org/10.1021/es103797z, 2011.
- Dong, P., Chen, Z., Qin, X., and Gong, Y.: Water significantly changes the ring-cleavage process during aqueous photooxidation of toluene, Environ. Sci. Technol., 55, 16316–16325, https://doi.org/10.1021/acs.est.1c04770, 2021.
- Dorfman, L. M., and Adams, G. E.: Reactivity of the hydroxyl radical in aqueous solutions, National Bureau of Standards, 76, 1973.
- Garmash, O., Rissanen, M. P., Pullinen, I., Schmitt, S., Kausiala, O., Tillmann, R., Zhao, D., Percival, C., Bannan, T. J., Priestley, M., Hallquist, Å. M., Kleist, E., Kiendler-Scharr, A., Hallquist, M., Berndt, T., McFiggans, G., Wildt, J., Mentel, T. F., and Ehn, M.: Multi-generation OH oxidation as a source for highly oxygenated organic molecules from aromatics, Atmos. Chem. Phys., 20, 515–537, https://doi.org/10.5194/acp-20-515-2020, 2020.
- Forstner, H. J. L., Flagan, R. C., and Seinfeld, J. H.: Secondary organic aerosol from the photooxidation of aromatic hydrocarbons: Molecular composition, Environ. Sci. Technol., 31, 1345–1358, https://doi.org/10.1021/es9605376, 1997.
- Gweme, D. T., and Styler, S. A.: OH radical oxidation of organosulfates in the atmospheric aqueous phase, J. Phys. Chem. A, 128, 9462–9475, https://doi.org/10.1021/acs.jpca.4c02877, 2024.
 - Hansen, A. M. K., Kristensen, K., Nguyen, Q. T., Zare, A., Cozzi, F., Nøjgaard, J. K., Skov, H., Brandt, J., Christensen, J. H., Ström, J., Tunved, P., Krejci, R., and Glasius, M.: Organosulfates and organic acids in Arctic aerosols: speciation, annual variation and concentration levels, Atmos. Chem. Phys., 14, 7807–7823, https://doi.org/10.5194/acp-14-7807-2014, 2014.
- Harrison, A. W., Waterson, A. M., and De Bruyn, W. J.: Spectroscopic and photochemical properties of secondary brown carbon from aqueous reactions of methylglyoxal, ACS Earth Space Chem., 4, 762–773, https://doi.org/10.1021/acsearthspacechem.0c00061, 2020.
 - He, J., Li, L., Li, Y., Huang, M., Zhu, Y., and Deng, S.: Synthesis, MS/MS characteristics and quantification of six aromatic organosulfates in atmospheric PM_{2.5}, Atmos. Environ., 290, 119361, https://doi.org/10.1016/j.atmosenv.2022.119361, 2022.
- Heath, A. A., Ehrenhauser, F. S., and Valsaraj, K. T.: Effects of temperature, oxygen level, ionic strength, and pH on the reaction of benzene with hydroxyl radicals in aqueous atmospheric systems, Environ. Chem. Eng., 1, 822–830, https://doi.org/10.1016/j.jece.2013.07.023, 2013.
 - Hems, R. F., and Abbatt, J. P. D.: Aqueous phase photo-oxidation of brown carbon nitrophenols: Reaction kinetics, mechanism, and evolution of light absorption, ACS Earth Space Chem., 2, 225–234,



405



- 390 https://doi.org/10.1021/acsearthspacechem.7b00123, 2018.
 - Herrmann, H., Schaefer, T., Tilgner, A., Styler, S. A., Weller, C., Teich, M., and Otto, T.: Tropospheric aqueous-phase chemistry: kinetics, mechanisms, and its coupling to a changing gas phase, Chem. Rev., 115, 4259–4334, https://doi.org/10.1021/cr500447k, 2015.
- Herrmann, H., Tilgner, A., Barzaghi, P., Majdik, Z., Gligorovski, S., Poulain, L., and Monod, A.: Towards a more detailed description of tropospheric aqueous phase organic chemistry: CAPRAM 3.0, Atmos. Environ., 39, 4351–4363, https://doi.org/10.1016/j.atmosenv.2005.02.016, 2005.
 - Herrmann, H., Hoffmann, D., Schaefer, T., Bräuer, P., and Tilgner, A.: Tropospheric aqueous-phase free-radical chemistry: Radical sources, spectra, reaction kinetics and prediction tools, ChemPhysChem, 11, 3796–3822, https://doi.org/10.1002/cphc.201000533, 2010.
- 400 Hettiyadura, A. P. S., Al-Naiema, I. M., Hughes, D. D., Fang, T., and Stone, E. A.: Organosulfates in Atlanta, Georgia: anthropogenic influences on biogenic secondary organic aerosol formation, Atmos. Chem. Phys., 19, 3191–3206, https://doi.org/10.5194/acp-19-3191-2019, 2019.
 - Hettiyadura, A. P. S., Jayarathne, T., Baumann, K., Goldstein, A. H., de Gouw, J. A., Koss, A., Keutsch, F. N., Skog, K., and Stone, E. A.: Qualitative and quantitative analysis of atmospheric organosulfates in Centreville, Alabama, Atmos. Chem. Phys., 17, 1343–1359, https://doi.org/10.5194/acp-17-1343-2017, 2017.
 - Hu, K. S., Darer, A. I., and Elrod, M. J.: Thermodynamics and kinetics of the hydrolysis of atmospherically relevant organonitrates and organosulfates, Atmos. Chem. Phys., 11, 8307–8320, https://doi.org/10.5194/acp-11-8307-2011, 2011.
 - Huang, L., Wang, Y., Zhao, Y., Hu, H., Yang, Y., Wang, Y., Yu, J-Z., Chen, T., Cheng, Z., Li, C., and Xiao., H.: Biogenic and anthropogenic contributions to atmospheric organosulfates in a typical megacity in eastern China, J GEOPHYS RES-ATMOS, 128, e2023JD038848, https://doi.org/10.1029/2023JD038848, 2023.
 - Iinuma, Y., Müller, C., Berndt, T., Böge, O., Claeys, M., and Herrmann, H.: Evidence for the existence of organosulfates from β-Pinene ozonolysis in ambient secondary organic aerosol, Environ. Sci. Technol., 41, 6678–6683, https://doi.org/10.1021/es070938t, 2007.
- Kuang, B. Y., Lin, P., Hu, M., and Yu, J., Z.: Aerosol size distribution characteristics of organosulfates in the Pearl River Delta region, China, Atmos. Environ.,130, 23–35, https://doi.org/10.1016/j.atmosenv.2015.09.024, 2016.
 - Kundu, S., Quraishi, T. A., Yu, G., Suarez, C., Keutsch, F. N., and Stone, E. A.: Evidence and quantitation of aromatic organosulfates in ambient aerosols in Lahore, Pakistan, Atmos. Chem. Phys., 13, 4865–4875, https://doi.org/10.5194/acp-13-4865-2013, 2013.
- Kwong, K. C., Chim, M. M., Davies, J. F., Wilson, K. R., and Chan, M. N.: Importance of sulfate radical anion formation and chemistry in heterogeneous •OH oxidation of sodium methyl sulfate, the smallest organosulfate, Atmos. Chem. Phys., 18, 2809–2820, https://doi.org/10.5194/acp-18-2809-2018, 2018.
 - Kristensen, K., and Glasius, M.: Organosulfates and oxidation products from biogenic hydrocarbons in fine aerosols from a forest in north west Europe during spring, Atmos. Environ., 45, 4546–4556,



430



- https://doi.org/10.1016/j.atmosenv.2011.05.063, 2011.
- 425 Lai, D., Schaefer, T., Zhang, Y., Li, Y. J., Xing, S., Herrmann, H., and Chan, M. N.: Deactivating effect of hydroxyl radicals reactivity by sulfate and sulfite functional groups in aqueous phase—atmospheric implications for small organosulfur compounds, ACS EST Air, 1, 678–689, https://doi.org/10.1021/acsestair.4c00033, 2024.
 - Lai, D., Bai, Y., Zhang, Z., So, P.-K., Li, Y. J., Tse, Y.-L. S., Yeung, Y.-Y., Schaefer, T., Herrmann, H., Yu, J. Z., Wang, Y., and Chan, M. N.: Rapid aqueous-phase oxidation of an α-pinene-derived organosulfate by hydroxyl radicals: a potential source of some unclassified oxygenated and small organosulfates in the atmosphere, Atmos. Chem. Phys., 25, 12569–12584, https://doi.org/10.5194/acp-25-12569-2025, 2025.
 - Laskin, A., Laskin, J., and Nizkorodov, S. A.: Chemistry of atmospheric brown carbon, Chem. Rev., 115, 4335–4382, https://doi.org/10.1021/cr5006167, 2015.
- Lay., T. H., Bozzelli, J. W., and Seinfeld, J. H.: Atmospheric photochemical oxidation of benzene: benzene + OH and the benzene-OH adduct (hydroxyl-2,4-cyclohexadienyl) + O₂, J. Phys. Chem., 100, 6543–6554, https://doi.org/10.1021/jp951726y, 1996.
 - Lei, Z., Chen, Y., Zhang, Y., Cooke, M. E., Ledsky, I. R., Armstrong, N. C., Olson, N. E., Zhang, Z., Gold, A., Surratt, J. D., and Ault, A. P.: Initial pH governs secondary organic aerosol phase state and morphology after uptake of isoprene epoxydiols (IEPOX), Environ. Sci. Technol., 56, 10596–10607, https://doi.org/10.1021/acs.est.2c01579, 2022.
- Li, F., Tsona, N. T., Li, J., and Du, L.: Aqueous-phase oxidation of syringic acid emitted from biomass burning: Formation of light-absorbing compounds, Sci. Total Environ., 765, 144239, https://doi.org/10.1016/j.scitotenv.2020.144239, 2021.
 - Li, S., Wang, Y., Zhang, Y., Yi, Y., Wang, Y., Guo, Y., Yu, C., Jiang, Y., Shi, J., Zhang, C., Zhu, J., Hu, W., Yu, J., Yao, X., Gao, H., and Hu, M.: Atmospheric organosulfate formation regulated by continental outflows and marine emissions over East Asian marginal seas, Atmos. Chem. Phys., 25, 12585–12598, https://doi.org/10.5194/acp-25-12585-2025, 2025.
- Li, X., Tao, Y., Zhu, L., Ma, S., Luo, S., Zhao, Z., Sun, N., Ge, X., and Ye, Z.: Optical and chemical properties and oxidative potential of aqueous-phase products from •OH and 3C*-initiated photooxidation of eugenol, Atmos. Chem. Phys., 22, 7793–7814, https://doi.org/10.5194/acp-22-7793-2022, 2022.
 - Liu, F., Xu, T., Ng, N. L., and Lu, H.: Linking cell health and reactive oxygen species from secondary organic aerosols exposure, Environ. Sci. Technol., 57, 1039–1048, https://doi.org/10.1021/acs.est.2c05171, 2022.
- Liu, G., Ji, J., Huang, H., Xie, R., Feng, Q., Shu, Y., Zhan, Y., Fang, R., He, M., Liu, S., Ye, X., and Leung, D. Y. C.: UV/H₂O₂:

 An efficient aqueous advanced oxidation process for VOCs removal, Chem. Eng. J., 324, 44–50, https://doi.org/10.1016/j.cej.2017.04.105, 2017.
 - Lin, Y.-H., Knipping, E. M., Edgerton, E. S., Shaw, S. L., and Surratt, J. D.: Investigating the influences of SO₂ and NH₃ levels on isoprene-derived secondary organic aerosol formation using conditional sampling approaches, Atmos. Chem. Phys., 13, 8457–8470, https://doi.org/10.5194/acp-13-8457-2013, 2013.
 - Lukács, H., Gelencsér, A., Hoffer, A., Kiss, G., Horváth, K., and Hartyáni, Z.: Quantitative assessment of organosulfates in size-segregated rural fine aerosol, Atmos. Chem. Phys., 9, 231–238, https://doi.org/10.5194/acp-9-231-2009, 2009.



465



- Ma, J., Reininger, N., Zhao, C, Döbler, D., Rüdiger, J., Qiu, Y., Ungeheuer, F., Simon, M., D'Angelo, L., Breuninger, A., David, J., Bai, Y., Li, Y., Xue, Y., Li, L., Wang, Y., Hildmann, S., Hoffmann, T., Liu, B., Niu, H., Wu, Z., and Vogel, A. L.:
 Unveiling a large fraction of hidden organosulfates in ambient organic aerosol, Nat. Commun., 16, 4098, https://doi.org/10.1038/s41467-025-59420-y, 2025.
 - Ma, Y., Xu, X., Song, W., Geng, F., and Wang, L.: Seasonal and diurnal variations of particulate organosulfates in urban Shanghai, China, Atmos. Environ., 85, 152–160, https://doi.org/10.1016/j.atmosenv.2013.12.017, 2014.
 - Mael, L. E., Jacobs, M. I., and Elrod, M. J.: Organosulfate and nitrate formation and reactivity from epoxides derived from 2-Methyl-3-buten-2-ol, J. Phys. Chem. A, 119, 4464–4472, https://doi.org/10.1021/jp510033s, 2015.
 - Minakata, D., Song, W., Mezyk, S. P., and Cooper, W. J.: Experimental and theoretical studies on aqueous-phase reactivity of hydroxyl radicals with multiple carboxylated and hydroxylated benzene compounds, Phys. Chem. Chem. Phys., 17, 11796–11812, https://doi.org/10.1039/C5CP00861A, 2015.
- Minerath, E. C., Casale, M. T., and Elrod, M. J.: Kinetics feasibility study of alcohol sulfate esterification reactions in tropospheric aerosols, Environ. Sci. Technol., 42, 4410–4415, https://doi.org/10.1021/es8004333, 2008.
 - Monod, A., and Doussin, J. F.: Structure-activity relationship for the estimation of OH-oxidation rate constants of aliphatic organic compounds in the aqueous phase: alkanes, alcohols, organic acids and bases, Atmos. Environ., 42, 7611-7622, https://doi.org/10.1016/j.atmosenv.2008.06.005, 2008.
 - Nozière, B., Ekström, S., Alsberg, T., and Holmström S.: Radical-initiated formation of organosulfates and surfactants in atmospheric aerosols, Geophys. Res. Lett., 37, L05806, https://doi.org/10.1029/2009GL041683, 2010.
 - Pan, X-M., Schuchmann, M. N., and Sonntag, C. V.: Oxidation of benzene by the OH radical. A product and pulse radiolysis study in oxygenated aqueous solution, J. Chem. Soc., Perkin Trans., 2, 289–297, https://doi.org/10.1039/P29930000289, 1993.
- Passananti, M., Kong, L., Shang, J., Dupart, Y., Perrier, S., Chen, J., Donaldson, J., and George, C.: Organosulfate formation through the heterogeneous reaction of sulfur dioxide with unsaturated fatty acids and long-chain alkenes, Angew. Chem. Int. Ed., 55, 10336-10339, https://doi.org/10.1002/anie.201605266, 2016.
 - Peng, X., Xie, T-T., Tang, M-X., Cheng, Y., Peng, Y., Wei, F-H., Cao, L-M., Yu, K., Du, K., He, L-Y., and Huang, X-F.: Critical role of secondary organic aerosol in urban atmospheric visibility improvement identified by machine learning, Environ. Sci. Technol. Lett., 10, 976–982, https://doi.org/10.1021/acs.estlett.3c00084, 2023.
- Riva, M., Chen, Y., Zhang, Y., Lei, Z., Olson, N. E., Boyer, H. C., Narayan, S., Yee, L. D., Green, H. S., Cui, T., Zhang, Z., Baumann, K., Fort, M., Edgerton, E., Budisulistiorini, S. H., Rose, C. A., Ribeiro, I. O., e Oliveira, R. L., dos Santos, E. O., Machado, C. M. D., Szopa, S., Zhao, Y., Alves, E. G., de Sá, S. S., Hu, W., Knipping, E. M., Shaw, S. L., Junior, S. D., de Souza, R. A. F., Palm, B. B., Jimenez, J-L., Glasius, M., Goldstein, A. H., Pye, H. O. T., Gold, A., Turpin, B. J., Vizuete, W., Martin, S. T., Thornton, J. A., Dutcher, C. S., Ault, A. P., and Surratt, J. D.: Increasing isoprene epoxydiol-to-inorganic sulfate aerosol ratio results in extensive conversion of inorganic sulfate to organosulfur forms: Implications for aerosol physicochemical properties, Environ. Sci. Technol., 53, 8682–8694, https://doi.org/10.1021/acs.est.9b01019,





2019.

- Schindelka, J., Iinuma, Y., Hoffmann, D., and Herrmann, H.: Sulfate radical-initiated formation of isoprene-derived organosulfates in atmospheric aerosols, Faraday Discuss., 165, 237–259, https://doi.org/10.1039/C3FD00042G, 2013.
- 495 Schuler, R. H., and Albarran, G.: The rate constants for reaction of radical •OH radicals with benzene and toluene, Radiat. Phys. Chem., 64, 189–195, https://doi.org/10.1016/S0969-806X(01)00497-2, 2002.
 - Shang, J., Passananti, M., Dupart, Y., Ciuraru, R., Tinel, L., Rossignol, S., Perrier, S., Zhu, T., and George, C.: SO₂ uptake on oleic acid: A new formation pathway of organosulfur compounds in the atmosphere, Environ. Sci. Technol. Lett., 3, 67–72, https://doi.org/10.1021/acs.estlett.6b00006, 2016.
- Shrivastava, M., Cappa, C. D., Fan, J., Goldstein, A. H., Guenther, A. B., Jimenez, J. L., Kuang, C., Laskin, A., Martin, S. T., Ng, N. L., Petaja, T., Pierce, J. R., Rasch, P. J., Roldin, P., Seinfeld, J. H., Shilling, J., Smith, J. N., Thornton, J. A., Volkamer, R., Wang, J., Worsnop, D. R., Zaveri, R. A., Zelenyuk, A., and Zhang, Q.: Recent advances in understanding secondary organic aerosol: Implications for global climate forcing, Rev. Geophys., 55, 509–559, https://doi.org/10.1002/2016RG000540, 2017.
- 505 Smith, J. D., Kinney, H., and Anastasio, C.: Aqueous benzene-diols react with an organic triplet excited state and hydroxyl radical to form secondary organic aerosol, Phys. Chem. Chem. Phys., 17, 10227–10237, https://doi.org/10.1039/C4CP06095D, 2015.
 - Surratt, J. D., Gómez-González, Y., Chan, A. W. H., Vermeylen, R., Shahgholi, M., Kleindienst, T. E., Edney, E. O., Offenberg, J. H., Lewandowski, M., Jaoui, M., Maenhaut, W., Claeys, M., Flagan, R. C., and Seinfeld, J. H.: Organosulfate formation in biogenic secondary organic aerosol, J. Phys. Chem. A, 112, 8345–8378, https://doi.org/10.1021/jp802310p, 2008.
 - Surratt, J. D., Chan, A. W. H., Eddingsaas, N.C., and Seinfeld, J. H.: Reactive intermediates revealed in secondary organic aerosol formation from isoprene, Proc. Natl. Acad. Sci. U.S.A., 107, 6640–6645, https://doi.org/10.1073/pnas.0911114107, 2010.
- Tang, S., Li, F., Tsona, N. T., Lu, C. Y., Wang, X. F., and Du, L.: Aqueous-phase photooxidation of vanillic acid: A potential source of Humic-Like Substances (HULIS), ACS Earth Space Chem., 4, 862–872, https://doi.org/10.1021/acsearthspacechem.0c00070, 2020.
 - Thomas, A. E., Glicker, H. S., Guenther, A. B., Seco, R., Vega Bustillos, O., Tota, J., Souza, R. A. F., and Smith, J. N.: Seasonal investigation of ultrafine-particle organic composition in an eastern Amazonian rainforest, Atmos. Chem. Phys., 25, 959–977, https://doi.org/10.5194/acp-25-959-2025, 2025.
- Tolocka, M. P., and Turpin, B.: Contribution of organosulfur compounds to organic aerosol mass, Environ. Sci. Technol., 46, 7978–7983, https://doi.org/10.1021/es300651v, 2012.
 - Wang, L., Wu, R., and Xu, C.: Atmospheric oxidation mechanism of benzene. fates of alkoxy radical intermediates and revised mechanism, J. Phys. Chem. A, 117, 14163–14168, https://doi.org/10.1021/jp4101762, 2013.
- Wang, S., Zhou, S., Tao, Y., Tsui, W. G., Ye, J., Yu, J.Z., Murphy, J. G., McNeill, V. F., Abbat, J. P. D., and Chan, A. W. H.:

 Organic peroxides and sulfur dioxide in aerosol: source of particulate sulfate, Environ. Sci. Technol., 53, 10695–10704,



530



- https://doi.org/10.1021/acs.est.9b02591, 2019.
- Wang, Y., Hu, M., Guo, S., Wang, Y., Zheng, J., Yang, Y., Zhu, W., Tang, R., Li, X., Liu, Y., Le Breton, M., Du, Z., Shang, D., Wu, Y., Wu, Z., Song, Y., Lou, S., Hallquist, M., and Yu, J.: The secondary formation of organosulfates under interactions between biogenic emissions and anthropogenic pollutants in summer in Beijing, Atmos. Chem. Phys., 18, 10693–10713, https://doi.org/10.5194/acp-18-10693-2018, 2018.
- Wang, Y., Ma, Y., Kuang, B., Lin, P., Liang, Y., Huang, C., and Yu, J. Z.: Abundance of organosulfates derived from biogenic volatile organic compounds: Seasonal and spatial contrasts at four sites in China, Sci. Total Environ., 806, 151275, https://doi.org/10.1016/j.scitotenv.2021.151275, 2022.
- Xu, R., Ge, Y., Kwong, K. C., Poon, H. Y., Wilson, K. R., Yu, J. Z., and Chan, M. N.: Inorganic sulfur species formed upon heterogeneous •OH oxidation of organosulfates: A case study of methyl sulfate, ACS Earth Space Chem., 4, 2041–2049, https://doi.org/10.1021/acsearthspacechem.0c00209, 2020.
 - Yao, M., Zhao, Y., Hu, M., Huang, D., Wang, Y., Yu, J. Z., and Yan, N.: Multiphase reactions between secondary organic aerosol and sulfur dioxide: kinetics and contributions to sulfate formation and aerosol aging, Environ. Sci. Technol. Lett., 6, 768–774, https://doi.org/10.1021/acs.estlett.9b00657, 2019.
- Yao, M., Zhao, Y., Chang, C. X., Wang, S., Li, Z., Li, C., Chan, A, W, H., and Xiao, H.: Multiphase reactions between organic peroxides and sulfur dioxide in internally mixed inorganic and organic particles: key roles of particle phase separation and acidity, Environ. Sci. Technol., 57, 15558–15570, https://doi.org/10.1021/acs.est.3c04975, 2023.
 - Yu, L., Smith, J., Laskin, A., Anastasio, C., Laskin, J., and Zhang, Q.: Chemical characterization of SOA formed from aqueous-phase reactions of phenols with the triplet excited state of carbonyl and hydroxyl radical, Atmos. Chem. Phys., 14, 13801–13816, https://doi.org/10.5194/acp-14-13801-2014, 2014.
- Zhang, H., Worton, D. R., Lewandowski, M., Ortega, J., Rubitschun, C. L., Park, J-H., Kristensen, K., Campuzano-Jost, P., Day, D. A., Jimenez, J. L., Jaoui, M., Offenberg, J. H., Kleindienst, T. E., Gilman, T. E., Gilman, J., Kuster, W. C., Gouw, J., Park, C., Schade, G. W., Frossard, A. A., Russell, L., Kaser, L., Jud, W., Hansel, A., Cappellin. L., Karl, T., Glasius, M., Guenther, A., Goldstein, A. H., Seinfeld, J. H., Gold, A., Kamens, R. M., and Surratt, J. D.: Organosulfates as tracers for secondary organic aerosol (SOA) formation from 2-Methyl-3-Buten-2-ol (MBO) in the atmosphere, Environ. Sci. Technol., 46, 9437–9446, https://doi.org/10.1021/es301648z, 2012.